Hindawi Publishing Corporation
Journal of Nanomaterials
Volume 2015, Article ID 171545, 9 pages
http://dx.doi.org/10.1155/2015/171545

Research Article

Enhancement of Gas Sensing Characteristics of Multiwalled Carbon Nanotubes by CF_4 Plasma Treatment for SF_6 Decomposition Component Detection

Xiaoxing Zhang,[1,2] Xiaoqing Wu,[1] Bing Yang,[3] and Hanyan Xiao[1]

[1]*State Key Laboratory of Power Transmission Equipment & System Security and New Technology, Chongqing University, Chongqing 400044, China*
[2]*School of Electrical Engineering, Wuhan University, Wuhan 430072, China*
[3]*Central Southern China Electric Power Design Institute, Wuhan 430071, China*

Correspondence should be addressed to Xiaoxing Zhang; xiaoxing.zhang@outlook.com

Received 2 July 2014; Accepted 30 November 2014

Academic Editor: Myoung-Woon Moon

H_2S and SO_2 are important gas components of decomposed SF_6 of partial discharge generated by insulation defects in gas-insulated switchgear (GIS). Therefore, H_2S and SO_2 detection is important in the state evaluation and fault diagnosis of GIS. In this study, dielectric barrier discharge was used to generate CF_4 plasma and modify multiwalled carbon nanotubes (MWNTs). The nanotubes were plasma-treated at optimum discharge conditions under different treatment times (0.5, 1, 2, 5, 8, 10, and 12 min). Pristine and treated MWNTs were used as gas sensors to detect H_2S and SO_2. The effects of treatment time on gas sensitivity were analyzed. Results showed that the sensitivity, response, and recovery time of modified MWNTs to H_2S were improved, but the recovery time of SO_2 was almost unchanged. At 10 min treatment time, the MWNTs showed good stability and reproducibility with better gas sensing properties compared with the other nanotubes.

1. Introduction

Sulfur hexafluoride (SF_6) is used as a gas medium in gas-insulated switchgear (GIS), which is widely used in substations and urban power grids because of its compact structure, high reliability, and low electromagnetic radiation [1, 2]. In the manufacture, transportation and installation processes inevitably lead to defects (e.g., metal burrs, protrusions, and suspended particles) in GIS equipment. Under long-term operation, these latent defects result in varying degrees of partial discharge (PD) that lead to SF_6 decomposition. Complex chemical reactions with trace amounts of air and water vapor in GIS generate SOF_2, SO_2F_2, SO_2, H_2S, and HF [3–6]. These by-products accelerate insulation aging and corrode metal surfaces, thereby yielding GIS faults [7]. H_2S and SO_2 are important gases of PD produced by latent insulation defects in GIS [8, 9]. Thus, H_2S and SO_2 detection is significant in the state evaluation and fault diagnosis of GIS equipment.

Products of SF_6 discharge decomposition are often detected using test tube method [10], gas chromatography [11], and infrared absorption spectrometry [12], but these techniques have several disadvantages. Carbon nanotubes (CNTs) are ideal materials for nanosized gas sensors because of their high surface adsorption capacity, good conductivity, and electronic transmission characteristics [13–17]. Analyses on CNT gas sensors have focused on the repeatability and the improvement of sensitivity. However, untreated CNTs are only sensitive to several gases (e.g., NH_3, NO_2, and H_2). Therefore, surface modification of CNTs should be explored to improve their sensitivity to other gases.

Gas discharge has been used to generate low-temperature plasma in material surface modification because of its low cost, efficiency, rapidity, and nonsignificant contribution to pollution. Dielectric barrier discharge (DBD) is employed to produce low-temperature plasma. The premodified materials are usually placed in the effective discharge area. O_2, N_2,

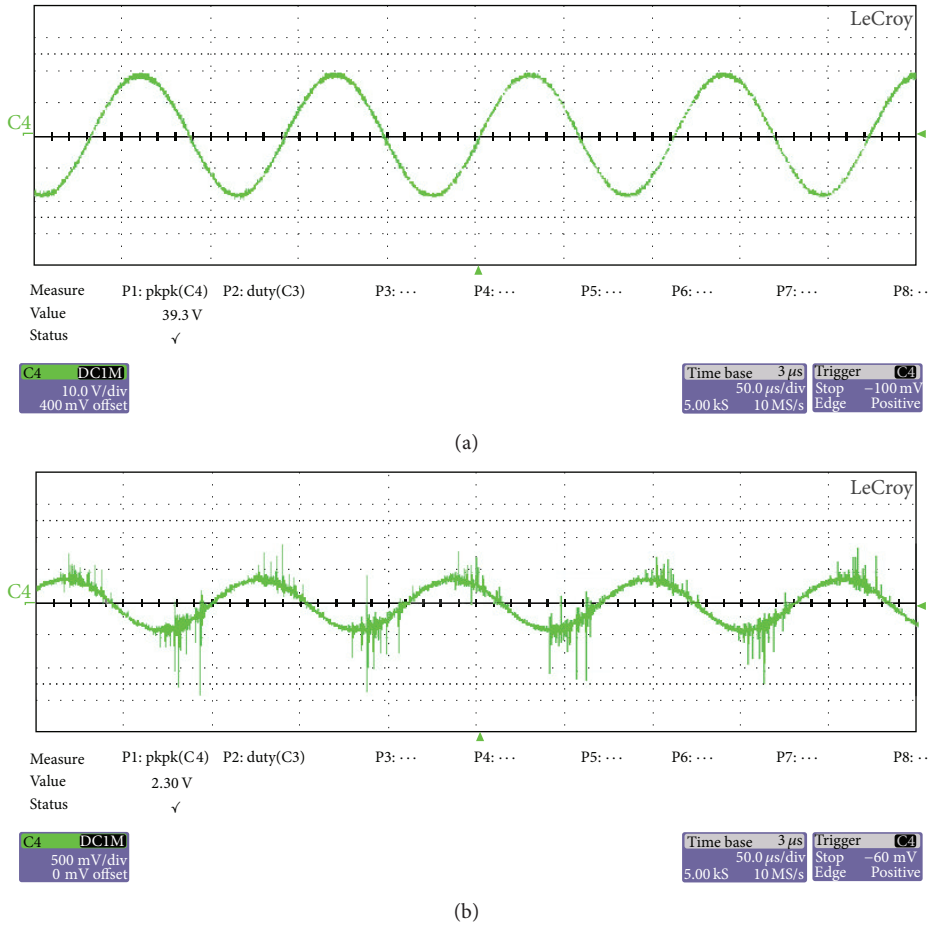

Figure 1: Discharge waveforms: (a) output voltage waveform and (b) output current waveform.

CF_4, and Ar, plasma, and so forth are used to etch the material surface, induce roughness, and connect the active groups. In 2010, Leghrib et al. reported that metal-doped O_2-plasma-treated multiwalled carbon nanotubes (MWNTs) exhibited high sensitivity to benzene vapor [18]. Dong et al. (2012) found that Ar- and O_2-plasma-modified CNTs have good responses to NO_2, whereas CF_4- and SF_6-treated CNTs are highly sensitive to NH_3 to achieve good selectivity [19]. In 2012, Zhang et al. used air-plasma-modified MWNTs that were generated by DBD under atmospheric pressure to detect H_2S and SO_2 [20]. They found that MWNTs-based gas sensors obtained higher responses to H_2S than those based on pristine nanotubes, but these sensors were not sensitive to SO_2.

CF_4 is a commonly used plasma etching gas. It is a kind of fluoride gas. In this study, the surface of the MWNTs is modified by CF_4 plasma generated by DBD. Then gas sensors based on MWNTs were fabricated to detect the products of SF_6 decomposition in GIS. Results showed that after plasma modification the sensitivity and response time of MWNTs gas sensors towards H_2S and SO_2 are greatly improved. MWNTs gas sensors with 10 min treatment time showed good stability and reproducibility with better gas sensing properties compared with other sensors.

2. Experiment

2.1. Surface Modification. MWNTs (tube diameter, 20 nm to 30 nm; length, 10 μm to 30 μm; purity, >95%) were grown by chemical vapor deposition (CVD) in black powder and purchased from the Chengdu Institute of Organic Chemistry Chengdu, China. CNTs are one-dimensional (1D) nanomaterials. Hence, appropriate surface processing parameters should be selected. Under strong plasma treatments, high power and long treatment time can destroy the tubular structure and carbonization of CNTs [21, 22]. In this study, a DBD plasma generator was used to modify MWNTs. Figure 1 shows the schematic for the test device. Low-temperature plasma experimental power (CTP-2000K) used in this experiment was produced from Nanjing Rongman Electronics Co., Ltd., China. The input voltage of the experimental power is controlled by a voltage regulator. Adjust the voltage to 30 V, which can be reading from the voltmeter (power input) in the power device. Adjust output frequency knob in the experimental power until frequency is around 10 kHz. Then we can get an optimum DBD discharge. Read the input current of 1.96 A from Ammeter in the power device. Use oscilloscope to obtain the output voltage and current waves, displayed in Figure 1. We should point out that there is

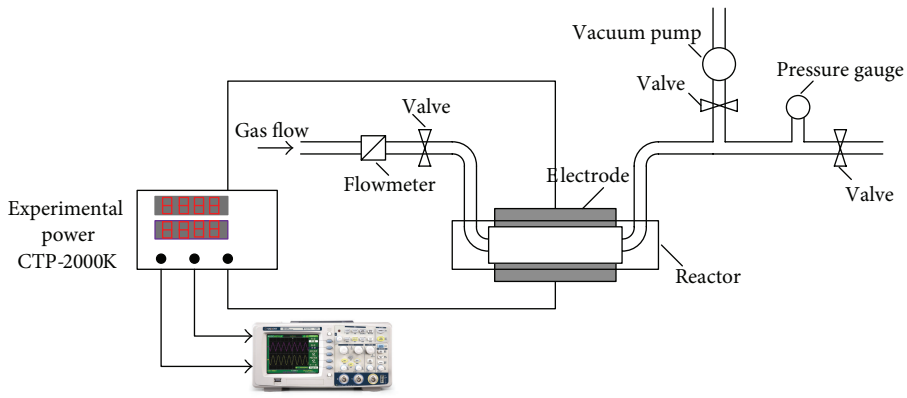

Figure 2: Schematic of the DBD experiment setup.

an attenuator in this experimental power and the attenuation coefficient is 1000. So the output peak-to-peak voltage is 39.3 kV. The discharge power in DBD plasma reactor can be calculated by Lissajou curve. However, due to the poor laboratory conditions we do not have enough oscilloscope attenuation probes to protect oscilloscope from breakdown. So other methods should be explored and we try to get in touch with the equipment manufacturers. According to the experience of the manufacturer's data, the plasma treatment power is approximately 0.8 times the input power at the same experimental conditions. Therefore, we can calculate the discharge power, which is 47 W.

Figure 2 reveals that the shape of the reactor is similar to a Petri dish. The reactor electrodes formed a parallel-plate structure and were made of 2 mm thick quartz glass. The upper and bottom electrodes were 8 mm apart. The bottom quartz glass electrode adhered to the reaction kettle, whereas the upper electrode is removable. In the modified experiment, an adequate amount of MWNTs was placed in a reaction kettle and sealed with silicone to ensure gas tightness. Air was released from the reactor to induce a vacuum state. CF_4 flow rate was controlled at 150 sccm. The parameters of the experimental power were adjusted, and MWNTs were, respectively, treated for 0.5, 1, 2, 5, 8, 10, and 12 min. The upper quartz glass was removed, and modified MWNTs were obtained after the treatment.

2.2. Preparation of MWNT Sensors. MWNT sensors were made of printed circuit board, and the substrate material is epoxy resin. Cu interdigital electrodes were etched in the substrate. The width and spacing of the electrodes are both 0.2 mm. First, MWNTs were placed into a beaker containing the appropriate ethanol solution. The beaker was placed in an ultrasonic bath for 1 h. Then, the sensor substrate was repeatedly cleaned with deionized water to remove impurities on the electrode surface. Next, the mixed solution was dropped on the substrate surface. Finally, the MWNT-coated substrates were baked in an oven at 80°C for a specific time. This process was repeated several times until uniform MWNTs films were deposited on the surface. Seven pristine and treated MWNTs with different modification times were used to fabricate the gas sensors.

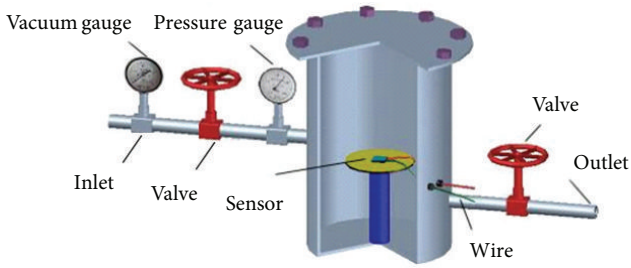

Figure 3: Structure of the gas sensor detecting device.

2.3. Sensitivity Measurement. Experiments on gas sensitivity were performed to test the resistance rate of the sensor upon exposure in the corresponding gas atmosphere. The gas sensing detection device mainly comprised a steel chamber, which was designed by our group and could be sealed by screws (Figure 3). The MWNTs sensors were placed in the gas chamber and connected to CHI660 electrochemical analyzer through the wires. The impedance-time function of the analyzer was used to record the changes in sensor resistance. Experiments were performed at room temperature.

Sensor sensitivity S is defined as

$$S = \frac{(R - R_0)}{R_0} \times 100\%, \quad (1)$$

where R represents the resistance upon exposure to the test gases and R_0 is the initial resistance of the sensor in vacuum.

For resistance-type sensors, the response time comes from the sensor in contact with target gas until 90% of the stable resistance is attained. The recovery time represents the speeds of gas desorption and is defined as the time by which the resistance returns to 90% of the initial value after escaping from the corresponding gas.

3. Results and Analysis

3.1. Fourier-Transform Infrared (FTIR) Spectrum. FTIR spectra are highly useful tools to analyze the characteristics of CNTs. Figure 4 shows the FTIR spectra of pristine MWNTs

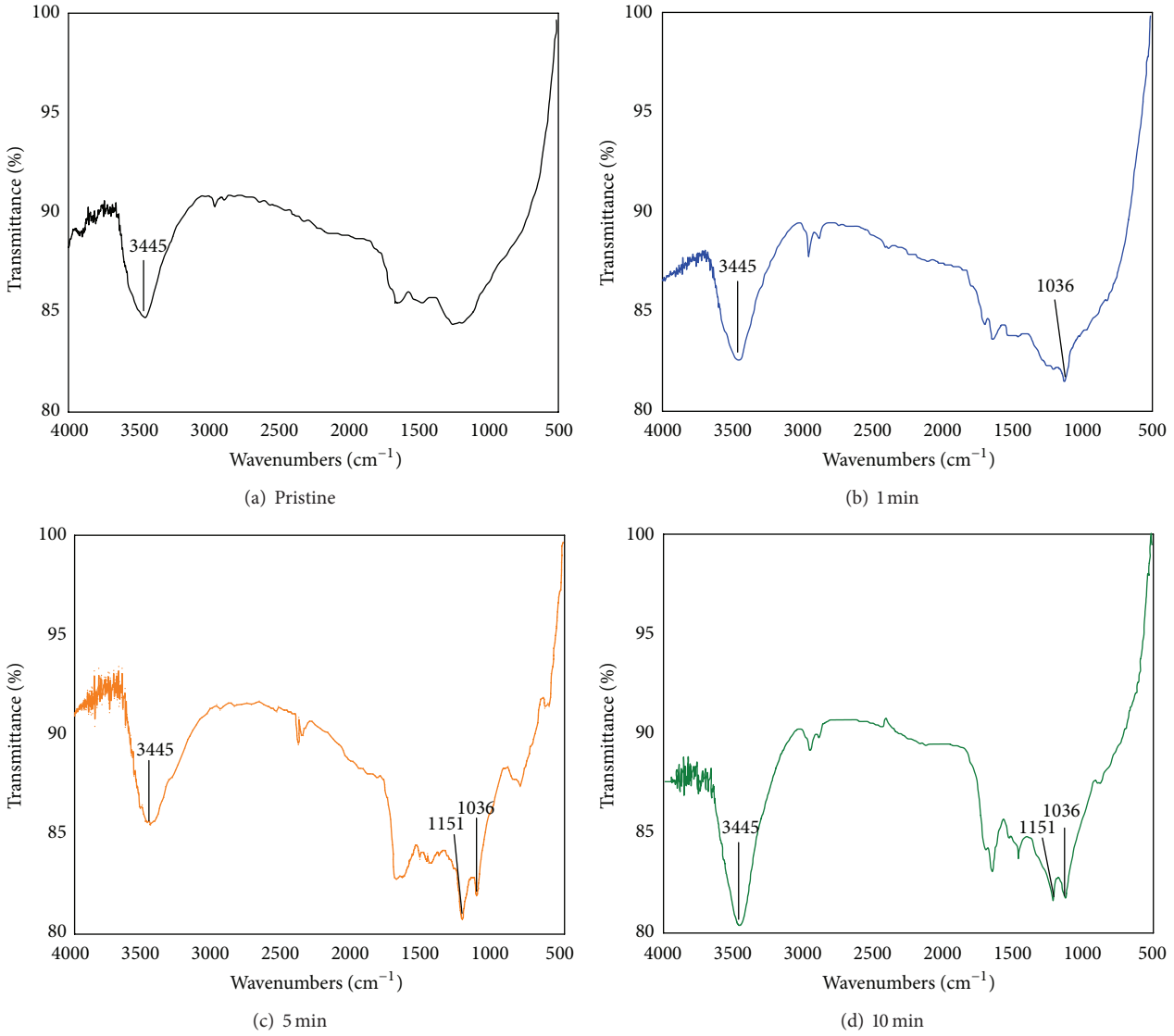

Figure 4: Infrared spectra of pristine and modified MWNTs.

and those generated by CF_4 plasma etching for 1, 5, and 10 min with a Nicolet 5DXC FT-IR spectrometer.

Diverse functional groups and types of bonding were observed in the FTIR spectra of MWNTs (Figure 4). The absorption peaks at 3445 cm^{-1} corresponded to the –OH groups in pristine and treated nanotubes. The absorption peaks at 1036 and 1151 cm^{-1} were ascribed to the respective C–F and symmetric –CF_2 stretching vibrations because of the CF_4-plasma treatment.

3.2. SEM Analysis. The surface morphologies of the pristine and plasma-treated MWNTs were analyzed using Zeiss Auriga focused ion beam and double-beam emission scanning electron microscopy (SEM). The SEM images of pristine MWNTs (Figure 5(a)) indicated the presence of several small particles, which included amorphous carbons and residual catalysts during preparation. Figures 5(b) and 5(c) show the SEM images of CF_4 plasma treated for 10 min. The impurities and dopant on the nanotube surfaces were removed, and MWNTs became shorter. Plasma treatment retained the nanotube structures.

3.3. Gas Sensing Properties of MWNTs Sensors to H_2S and SO_2. We used eight kinds of MWNTs-based gas sensors (pristine MWNTs and MWNTs modified by plasma for different time) to detect H_2S and SO_2 whose concentrations are 50 ppm for them both. The gas response curves are shown in Figure 6. It can be seen from Figures 6(a) and 6(b) that the sensitivity of pristine MWNTs and those modified by CF_4 plasma for 0.5, 1, and 2 min to H_2S are 3%, 3.2%, 3.4%, and 3.5%, respectively, and to SO_2 are 2.3%, 2.4%, 2.6%, and 2.7%. Obviously, after modification the gas sensitivities of MWNTs are not markedly enhanced. Under small discharge power, these phenomena may have been caused by the insufficient treatment time and poor surface modification. Therefore, if the discharge power remains unchanged, in order to achieve

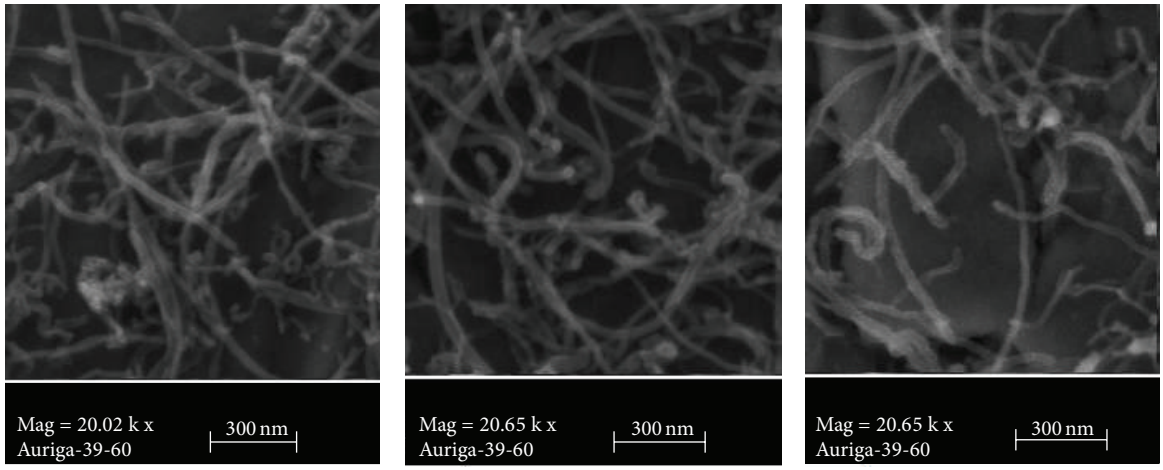

Figure 5: SEM images: (a) pristine and (b and c) modified MWNTs for 10 min.

a better surface modification plasma treatment time should be extended.

In consequence, Figures 6(c) and 6(d) show the response curves of pristine MWNTs and these treated for 5, 8, 10, and 12 min to H_2S and SO_2. We can see that when the treatment time is less than 10 min, the sensitivities of MWNTs sensors increased with increasing of treatment time. Meanwhile, the MWNTs modified by CF_4 plasma for 10 min exhibited the best sensitivity to both H_2S and SO_2. However, the sensitivities decreased when the treatment time is over 10 min. Possible reasons may be that after longer treatment time the structure of the nanotubes was destroyed and nanotubes were partly carbonized [21] under the bombardment of energetic particles in prolonged plasma treatments, which result in a reduction of active adsorption sites on MWNTs surface for gas molecules. Hence, the gas sensing properties of the MWNTs were affected.

Figure 6 reveals that the response time of CF_4 plasma-modified MWNTs sensors to H_2S and SO_2 was shorter. For treatment times ranging from 0 min to 10 min, the response time decreased with increasing treatment time. Besides, the shortest response times to H_2S and SO_2 are 70 and 150 s, respectively.

3.4. Responses of MWNTs-Based Sensors to H_2S and SO_2 at Different Concentrations. MWNT sensors modified by CF_4 plasma for 10 min (Section 3.3) were selected to detect H_2S and SO_2 at 10, 25, 50, and 100 ppm because these sensors yielded the best sensitivities. Figures 7(a) and 7(b) indicate that the sensitivity of the sensors increases with the gas concentration.

Figure 8 shows that the gas concentration and sensor sensitivity were linearly correlated for H_2S and SO_2 concentrations of 10 ppm to 100 ppm with correlation coefficients (R^2) of 0.97183 and 0.9739, respectively.

3.5. Desorption and Repeatability of MWNTs-Based Sensors. To analyze the desorption properties of modified MWNTs gas sensors, these modified by CF_4 plasma for 10 min were chosen to test the recovery curve, as shown in Figure 9. The experiment steps are as follows. Firstly, the chamber was pumped into vacuum and was standing for a period of time. After resistance of the sensor remains unchanged, in the second minute 50 ppm H_2S was introduced into the chamber and the resistance showed a quick decrease. Few minutes later, the resistance of sensor remains stable. Currently, H_2S gas molecules reach adsorption equilibrium at the surface of MWNTs. In the fifth minute, pure N_2 was injected into the gas chamber, and the sensor resistance can generally recover near the initial value. There is still a small amount of residual gas accumulating on the surface of the sensor which affects the sensitivity. In order to obtain a complete desorption, place the sensor under UV irradiation. By irradiating with UV light, the residual gas absorbs energy, which enables it to "escape" from the "trapped" state where almost no residual gas remains on the surface of the tested sensor. After N_2 and UV treatments, the sensor resistance was gradually restored to its initial value. The recovery time was about 25 min, which was less than that of the pristine MWNTs sensor to H_2S (40 min; data not shown).

The MWNTs sensor modified by plasma for 10 min that was most sensitive to SO_2 was selected to illustrate the repeatability process (Figure 10). The resistance-change trends remained similar, and the maximum resistance-change rate remained the same and stable. Hence, the gas sensor could be repeatedly used with good response and stability. However, the recovery time was approximately 35 min and was not greatly enhanced in contrast to that of pristine MWNT-based sensors.

3.6. Gas Sensing Mechanism. The CF_4-plasma-modified MWNTs sensors exhibited high sensitivities to H_2S and SO_2 because of the following reasons: (1) the accelerated electrons, ions, and free radicals cleaned the MWNT surface by etching some amorphous carbon and catalyst particles during plasma treatment; (2) the bombardment of energetic particles

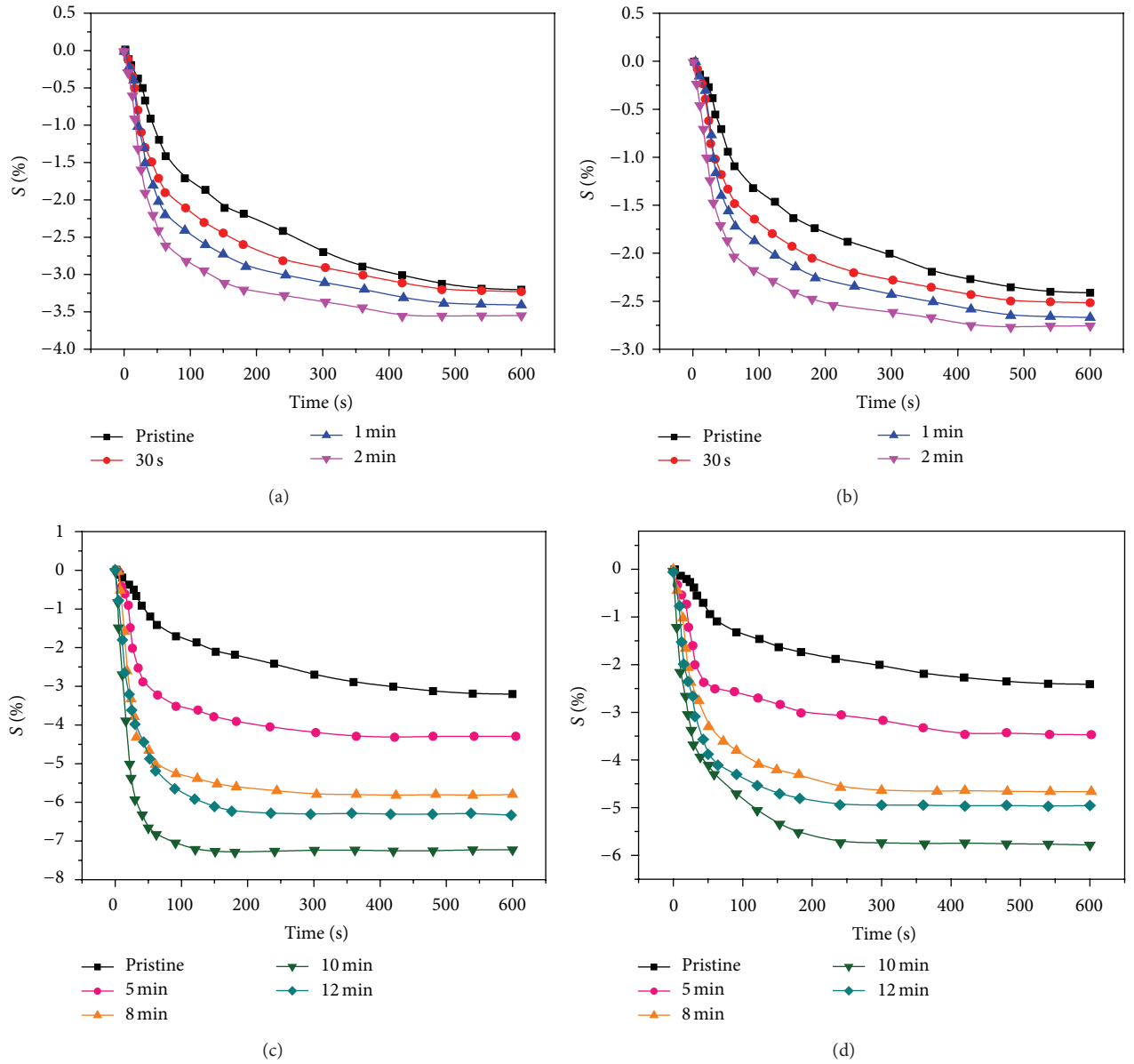

Figure 6: Responses of MWNTs-based gas sensors: (a, c) 50 ppm H_2S and (b, d) 50 ppm SO_2.

destroyed some of the nanotubes and increased the defects on their surfaces, which generated effective adsorption sites for gas molecules; and (3) CF_4, a fluorinated gas [22], was ionized to generate fluoride ions in DBD and react with carbon atoms on the MWNTs surface to yield C–F bonds [23] without destroying the tubular structure. Given the strong polarity and reactivity of F atoms, fluorinated MWNTs exhibited strong adsorption capacities and high gas sensing properties.

The response and recovery time of plasma-modified MWNT sensors to H_2S were remarkably reduced, but only the response time to SO_2 decreased, and recovery time was not reduced (Section 3.5). Theoretically, H_2S molecules were physically adsorbed on the surface of MWNTs through van der Waals interaction. However, some hydroxyls existed on the surfaces of the nanotubes during growth by CVD. F atoms were introduced onto the MWNTs surface after fluorination. C–F bonds possessed high polarity because of the strong electronegativity of the F atom, during which –F was essential. Stable hydrogen bonds (C–F$\cdots$H–S) were formed between H atoms in H_2S molecules and F atoms when H_2S molecules were adsorbed on the surface of modified MWNTs. Subsequently, the van der Waals forces were replaced, and the adsorption of H_2S molecules was accelerated to reduce the response time (Figure 11(a)). In addition, O atoms in the hydroxyl groups in MWNTs surfaces exhibited small atomic radii and high electronegativities. Hydrogen bonds (C–O$\cdots$H–S) were formed between O atoms in hydroxyl and H atoms in H_2S molecules (Figure 11(a)). The recovery time of plasma-based MWNTs sensors to H_2S decreased possibly because of the effect of UV irradiation that the H–F

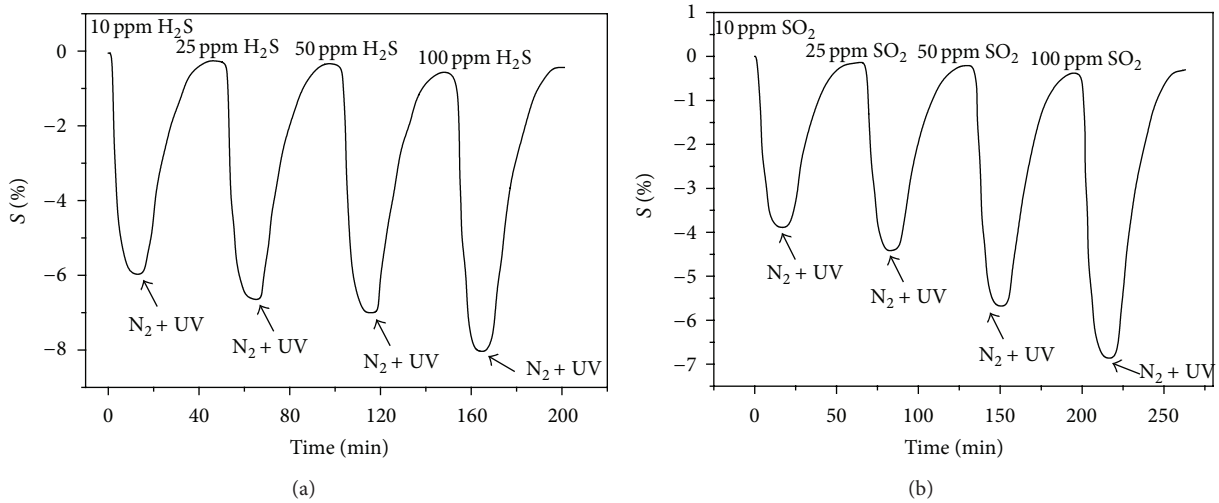

Figure 7: Response curves of MWNTs-based sensors to different concentrations of (a) H_2S and (b) SO_2.

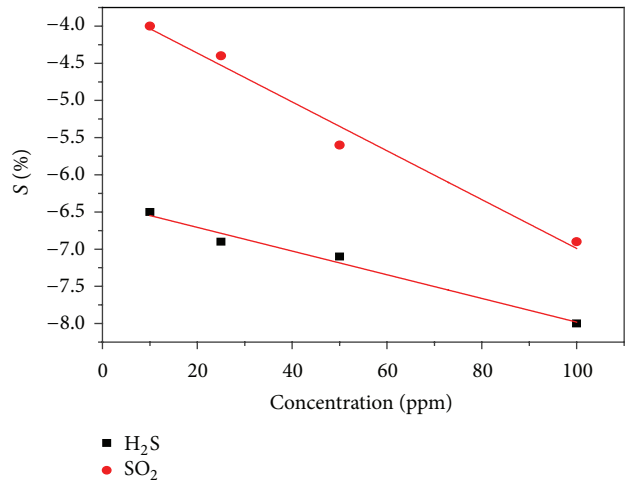

Figure 8: Linear relationship sensitivity of MWNT-based sensors for different concentrations of SO_2 and H_2S.

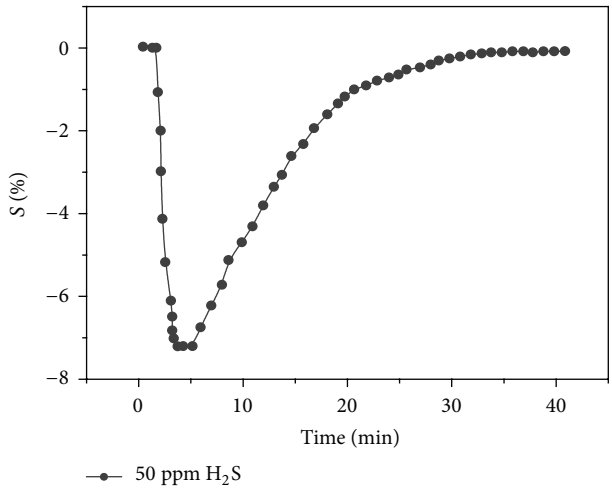

Figure 9: Recovery curve of plasma-modified MWNTs to H_2S.

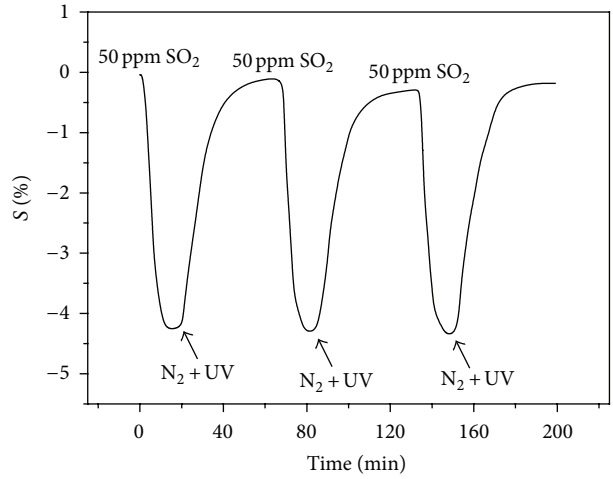

Figure 10: Reversibility curve of modified MWNTs to 50 ppm SO_2.

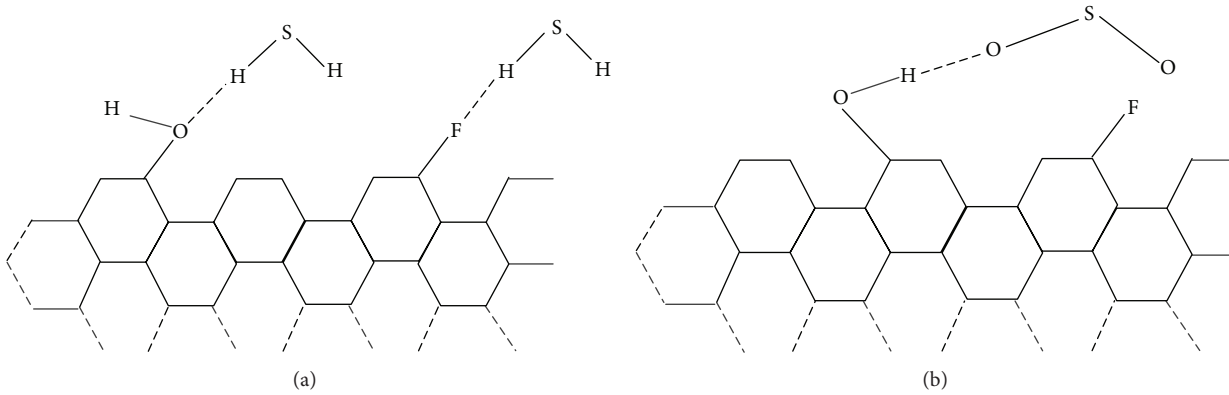

(a) (b)

Figure 11: Schematic of the absorption of (a) H_2S and (b) SO_2 in modified MWNTs.

bond is easier to disintegrate. For SO_2, only O atoms in the SO_2 molecules and H atoms of hydroxyl were combined to form hydrogen bonds (O–H$\cdots$O–S; Figure 11(b)). F atoms on the surfaces of modified MWNT increased the number of effective adsorption sites for gas molecules, accelerated the adsorption, and reduced the response time. However, the recovery time remained invariant.

4. Conclusions

MWNTs were modified by DBD CF_4 plasma for 0.5, 1, 2, 5, 8, 10, and 12 min. The gas sensitivities of the treated MWNTs sensors to H_2S and SO_2 were evaluated. The following conclusions were drawn.

(1) Modification effects were closely related to the treatment time under a small plasma discharge power. The gas sensitivities of MWNTs did not improve significantly under short treatment times compared with those of pristine counterparts.

(2) For <10 min treatment times, the sensitivities of MWNT sensors increased with the treatment time. MWNTs treated for 10 min exhibited the best sensitivity to H_2S and SO_2 with good recovery and stability.

(3) SEM micrographs and FTIR analyses of pristine and modified MWNTs revealed that modified MWNTs contained a low number of impure particles on the surface as well as short length and grafted –F polar functional groups. Hence, gas adsorption was highly convenient for the nanotubes, and gas sensitivity was improved.

Conflict of Interests

The authors declare that there is no conflict of interests regarding the publication of this paper.

Acknowledgments

The authors gratefully acknowledge the financial support from National Natural Science Foundation of P. R. China (Project no. 51277188), New Century Excellent Talents in University Program (NCET-12-0590), and Project Supported by the Funds for Innovative Research Groups of China (51321063).

References

[1] Y. Martin, Z. Li, T. Tsutsumi et al., "Detection of SF_6 decomposition products generated by DC corona discharge using a carbon nanotube gas sensor," *IEEE Transactions on Dielectrics and Electrical Insulation*, vol. 19, no. 2, pp. 671–676, 2012.

[2] X. Zhang, J. Ren, J. Tang, and C. Sun, "Kernel statistical uncorrelated optimum discriminant vectors algorithm for GIS PD recognition," *IEEE Transactions on Dielectrics and Electrical Insulation*, vol. 16, no. 1, pp. 206–213, 2009.

[3] C. Beyer, H. Jenett, and D. Klockow, "Influence of reactive SF_x gases on electrode surfaces after electrical discharges under SF_6 atmosphere," *IEEE Transactions on Dielectrics and Electrical Insulation*, vol. 7, no. 2, pp. 234–240, 2000.

[4] M. Piemontesi and L. Niemeyer, "Sorption of SF_6 and SF_6 decomposition products by activated alumina and molecular sieve 13X," in *Proceedings of the IEEE International Symposium on Electrical Insulation*, pp. 828–838, IEEE, Quebec, Canada, June 1996.

[5] X. X. Zhang, W. T. Liu, J. Tang, and P. Xiao, "Study on PD detection in SF_6 using multi-wall carbon nanotube films sensor," *IEEE Transactions on Dielectrics and Electrical Insulation*, vol. 17, no. 3, pp. 833–838, 2010.

[6] R. J. Van Brunt, "Production rates for oxy-fluorides SOF_2, SO_2F_2 and SOF_4 in SF_6 corona discharges," *Journal of Research of the National Bureau of Standards*, vol. 90, no. 3, pp. 229–253, 1985.

[7] J. M. Braun, F. Y. Chu, and R. Seethapathy, "Characterization of GIS spacers exposed to SF_6 decomposition products," *IEEE transactions on electrical insulation*, vol. 22, no. 2, pp. 187–193, 1986.

[8] X.-X. Zhang, Y. Yao, J. Tang, C.-X. Sun, and L.-Y. Wan, "Actuamity and perspective of proximate analysis of SF_6 decomposed products under partial discharge," *High Voltage Engineering*, vol. 34, no. 4, pp. 664–747, 2008.

[9] X. X. Zhang, C. C. Luo, and J. Tang, "Sensitivity characteristic analysis of adsorbent-mixed carbon nanotube sensors for the detection of SF_6 decomposition products under PD conditions," *Sensors (Switzerland)*, vol. 13, no. 11, pp. 15209–15220, 2013.

[10] I. A. Metwally, "Status review on partial discharge measurement techniques in gas-insulated switchgear/lines," *Electric Power Systems Research*, vol. 69, no. 1, pp. 25–36, 2004.

[11] A. Derdouri, J. Casanovas, R. Hergli, R. Grob, and J. Mathieu, "Study of the decomposition of wet SF_6, subjected to 50-Hz ac corona discharges," *Journal of Applied Physics*, vol. 65, no. 5, pp. 1852–1857, 1989.

[12] H. M. Heise, R. Kurte, P. Fischer, D. Klockow, and P. R. Janissek, "Gas analysis by infrared spectroscopy as a tool for electrical fault diagnostics in SF_6 insulated equipment," *Fresenius' Journal of Analytical Chemistry*, vol. 358, no. 7-8, pp. 793–799, 1997.

[13] C. T. White and T. N. Todorov, "Carbon nanotubes as long ballistic conductors," *Nature*, vol. 393, no. 6682, pp. 240–241, 1998.

[14] P. G. Collins, K. Bradley, M. Ishigami, and A. Zettl, "Extreme oxygen sensitivity of electronic properties of carbon nanotubes," *Science*, vol. 287, no. 5459, pp. 1801–1804, 2000.

[15] P. Qi, O. Vermesh, M. Grecu et al., "Toward large arrays of multiplex functionalized carbon nanotube sensors for highly sensitive and selective molecular detection," *Nano Letters*, vol. 3, no. 3, pp. 347–351, 2003.

[16] J. Kong, N. R. Franklin, C. Zhou et al., "Nanotube molecular wires as chemical sensors," *Science*, vol. 287, no. 5453, pp. 622–625, 2000.

[17] P. Slobodian, P. Riha, A. Lengalova, P. Svoboda, and P. Saha, "Multi-wall carbon nanotube networks as potential resistive gas sensors for organic vapor detection," *Carbon*, vol. 49, no. 7, pp. 2499–2507, 2011.

[18] R. Leghrib, A. Felten, F. Demoisson, F. Reniers, J.-J. Pireaux, and E. Llobet, "Room-temperature, selective detection of benzene at trace levels using plasma-treated metal-decorated multi-walled carbon nanotubes," *Carbon*, vol. 48, no. 12, pp. 3477–3484, 2010.

[19] K.-Y. Dong, D.-J. Ham, B. H. Kang et al., "Effect of plasma treatment on the gas sensor with single-walled carbon nanotube paste," *Talanta*, vol. 89, pp. 33–37, 2012.

[20] X. X. Zhang, B. Yang, X. J. Wang, and C. C. Luo, "Effect of plasma treatment on multi-walled carbon nanotubes for the detection of H_2S and SO_2," *Sensors (Switzerland)*, vol. 12, no. 7, pp. 9375–9385, 2012.

[21] A. Felten, C. Bittencourt, J. J. Pireaux, G. van Lier, and J. C. Charlier, "Radio-frequency plasma functionalization of carbon nanotubes surface O_2, NH_3, and CF_4 treatments," *Journal of Applied Physics*, vol. 98, no. 7, Article ID 074308, 2005.

[22] L. Valentini, D. Puglia, I. Armentano, and J. M. Kenny, "Sidewall functionalization of single-walled carbon nanotubes through CF_4 plasma treatment and subsequent reaction with aliphatic amines," *Chemical Physics Letters*, vol. 403, no. 4–6, pp. 385–389, 2005.

[23] Y. M. Shulga, T.-C. Tien, C.-C. Huang et al., "XPS study of fluorinated carbon multi-walled nanotubes," *Journal of Electron Spectroscopy and Related Phenomena*, vol. 160, no. 1–3, pp. 22–28, 2007.